Satellite Mega-constellation Monitoring Campaign Using the VGOS Radio Telescope at Yebes Observatory during a 24-hour VLBI Session of the IVS

Marta Bautista Durán[1], Jose A. López-Pérez[1], Javier González[1], Federico di Vruno[2], Benjamin Winkel[3]

Abstract In recent years, the number of satellites in low earth orbit (LEO) has increased exponentially due to the so-called "mega-constellations." The impact of this large number of satellites crossing the sky during geodetic VLBI observations is still not clear. For example, some studies have been carried out to determine whether the VGOS radio telescope could be driven into saturation mode or, even worse, destroyed. The current scenario (around five thousand of these satellites in the sky) is better than the one expected in the next decade, where the number of these satellites would be around a hundred thousand. The aim of this work is to evaluate the current impact and the number of satellites detected during a typical 24-hour observing session of the IVS using the VGOS telescope at Yebes.

1 Introduction

In recent years, the number of satellites orbiting the Earth has increased. Most of them are part of so-called mega-constellations (operating in LEO). This will have an impact on both optical and radio astronomy observations. The most popular example of these satellites is Starlink (with 4,400 satellites in its first phase) or OneWeb (with 648 satellites in its first phase). So far, most Internet communications satellites have been positioned in geostationary orbit (GEO) [1]. The difference from the point of view of radio telescopes is that these satellites are stationary and located in a limited area, whereas LEO satellites are spread across the whole sky. The exponential growth in the number of active satellites in low Earth orbit could result in more than 2,000 satellites above the local horizon at any given time [1].

A typical 24-hour geodetic VLBI observing session is optimized so that the sky distribution of observations at each station is as uniform as possible in all directions, while maintaining mutual visibility with as many telescopes in the network as possible (see Figure 2). The frequency bands that are currently used by the IVS are the following [2]:

- A-band: 3,000.4 – 3,480.4 MHz
- B-band: 5,240.4 – 5,720.4 MHz
- C-band: 6,360.4 – 6,840.4 MHz
- D-band: 10,200.4 – 10,680.4 MHz

An emerging threat to VGOS is the operation of mega-constellations in the 10.75–12.75 GHz downlink range. Some GSO satellites also operate in the same frequency range.

In this work, the VGOS telescope at Yebes was used to monitor the four bands (A, B, C, and D). The D-band is adjacent to the frequency used by mega-constellations (10.7–12.7 GHz). With the help of an RFI measurement setup, the mega-constellation frequency range is measured to evaluate the impact that these emissions could produce on the D-band of the VGOS observations.

The monitoring measurements were carried out during several VLBI sessions, using a copy of the receiver outputs (2–14 GHz) analyzed with the RFI equipment. Here we only present the results of a session observed on 26 July 2023.

1. Yebes Observatory (IGN), Yebes, Spain
2. SKA Observatory, Jodrell Bank, Manchester, United Kingdom
3. Max-Planck-Institut für Radioastronomie, Bonn, Germany

1.1 Monitoring System Setup

The RFI monitoring system consisted of a power splitter, a band-pass filter, and a spectrum analyzer (SA), as seen in the gray boxes in Figure 1.

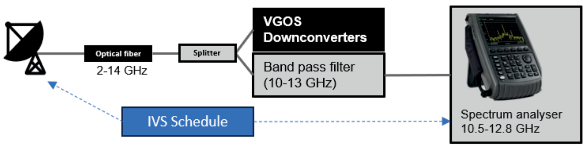

Fig. 1 Monitoring setup used for RFI detection measurements.

To monitor the spectrum at the VGOS antenna, the splitter was placed at the output of the optical fiber link receiver to get a copy of the whole band (2–14 GHz). To avoid possible saturation at the SA, a band-pass filter (10–13 GHz) was placed between the splitter and the SA. The model of SA used was the hand-held Keysight N9962A.

Data acquisition is synchronized with the IVS session through the schedule provided in advance by the operator so that the spectrum analyzer data is received at the same time as the scans. The schedule includes the scan number, azimuth and elevation, start time, stop time, and observation duration for each scan. The spectrum analyzer is configured in max-hold mode for the duration of each scan (30 seconds).

Table 1 gives an example of the information from an IVS schedule summarizing the fields required for the monitoring campaign.

Table 1 Information from a sample schedule of an IVS session.

Scan	Azimuth	Elevation	Start (UTC)	Stop (UTC)	Duration (s)
194-1800b	201.0	60.0	18:00:00	18:00:30	0:30
194-1801a	33.0	72.0	18:01:08	18:01:38	0:30
194-1802	261.0	16.0	18:02:16	18:02:46	0:30
194-1803b	2.0	9.0	18:03:45	18:04:15	0:30
194-1804	97.0	22.0	18:04:53	18:05:23	0:30

2 RFI Measurements

The following evaluation corresponds to VGOS-OPS session vo3207 (26-07-2023). The SA is configured in max-hold mode with the detector in averaging mode for the duration of each scan. Once the scan is complete, the trace is stored in a .csv file with information on the antenna position and the time period of the scan. At the end of the 24-hour session, a total of 1080 scans had been measured and recorded with the SA.

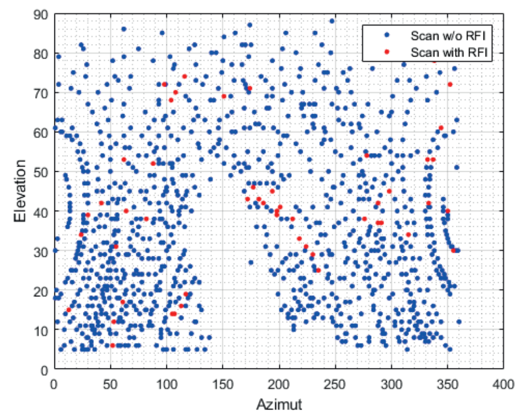

Fig. 2 Total number of scans during vo3207 (26-07-2023). The scans without the presence of RFI are shown in blue; otherwise, in red.

Once the IVS session is complete, the data is analyzed first to determine which scans contain satellite signals and then to try to find the sources of the signals. The post-processing is explained in detail in the following section.

3 Data Processing

At the end of the IVS session, the data recorded with the SA are processed to analyze the number of scans with satellite signals (SS), the number of satellites crossing the antenna beam during each scan, and the effect that these satellites could have on the VGOS observations, comparing the system noise temperature (T_{sys}) under different circumstances.

3.1 RFI Detection

The first step is to evaluate the data obtained with the SA to analyze which scans contain any presence of satellite signals. A dataset containing this information is then produced.

This is done by applying some simple statistics to the data (mean, standard deviation). Figure 2 shows the different positions (scans) on the sky covered during a particular IVS session (26-07-2023). The positions without the presence of SS are shown in blue, and those with the presence of SS are shown in red. Figure 3 shows an example of a scan with a satellite signal.

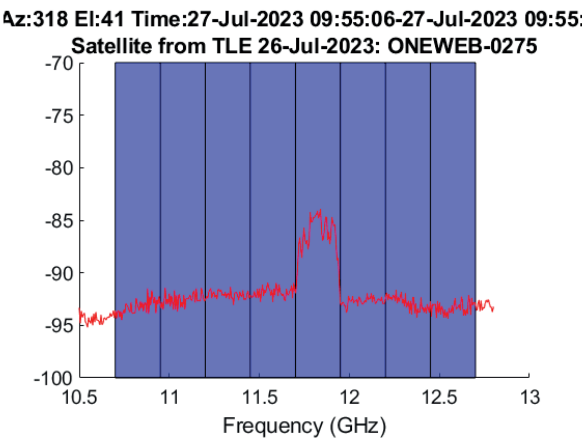

Fig. 3 Sample scan with the presence of a OneWeb satellite signal. The different sub-bands of the non geo-satellites (10.7–12.7 GHz) are in blue.

3.2 Satellite Detector

Python software has been developed to obtain the list of satellites (Starlink, OneWeb, and geostationary) crossing the sky around the antenna at a given time (between the start and stop times from the schedule) and at the position of each scan. Figure 4 shows an example of a typical scenario based on the current deployment of different types of satellites (Starlink, OneWeb, and geostationary). Information on the TLEs has been derived from a database created by SKAO (M. D'Cruze, B. Sorokin). The beamwidth of the antenna at half power at 11 GHz is 0.14°. Due to the high sensitivity of the antenna, it is very likely that the antenna receives the satellite signals through its secondary lobes, so other beamwidth values are evaluated [3]. The sizes evaluated in this report are 0.14°, 1°, 2°, and 4°.

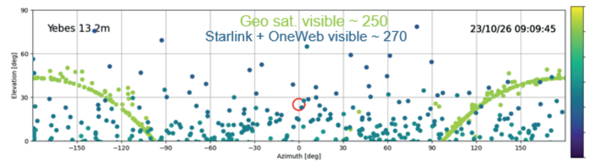

Fig. 4 Typical satellite deployment scenario (Starlink, OneWeb, and geostationary satellites) seen with the VGOS telescope at Yebes.

The software uses the TLEs and the Python package *cysgp4* to propagate the TLEs to the specific time of each scan (the closest TLE in time is chosen for greater accuracy). The output is a `.txt` file containing the satellite list with the NORAD names of the satellites and the time of the pass. Once this information is known, the scans with SS can be associated with their possible source.

3.3 Associate RFI Scan with Satellite Source

To evaluate the number of satellites passing through the field of view of the VGOS antenna, different values of beam size are evaluated. Figures 5–7 show the different situations depending on the beam size of the antenna. Table 2 summarizes the number of potential detections associated with the type of satellite. In this table, columns 2, 4, and 6 show the number of satellites crossing each beam (column 1) derived from the TLEs. Columns 3, 5, and 7 show the number of SS detected at the spectrum analyzer. Column 8 represents the number of RFI detections without any associated source.

4 Evaluation of the System Temperature of D-band

The final step in this study is to evaluate the potential impact of signals from different satellites on the system noise temperature (T_{sys}) in the adjacent band (D-band, 10.2–10.68 GHz). T_{sys} is evaluated every second dur-

Table 2 Potential detections of satellites for each beam size case.

Beam size (°)	# Starlinks from TLEs	# Starlinks detected	# Onewebs from TLEs	# Oneweb detected	# GEO sats. from TLEs	# GEO sats. detected	RFI detected w/o associated source
0.14	13	2	0	0	0	0	81
1	78	18	9	1	11	7	58
2	159	26	19	3	25	17	41
4	321	40	47	4	76	42	11
8	578	60	137	11	121	45	3

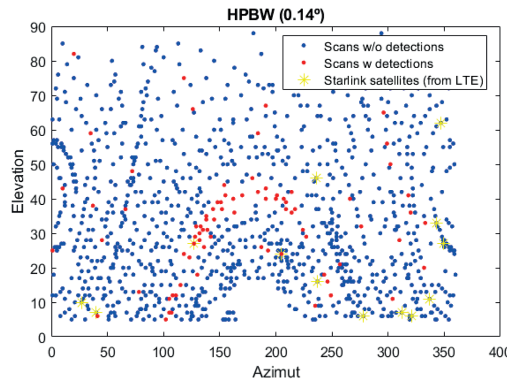

Fig. 5 Total number of scans (in blue: scans without SS; in red: those with SS). Those scans with the presence of a Starlink satellite crossing the 0.14° beam during the 30-second duration of the scan are in yellow.

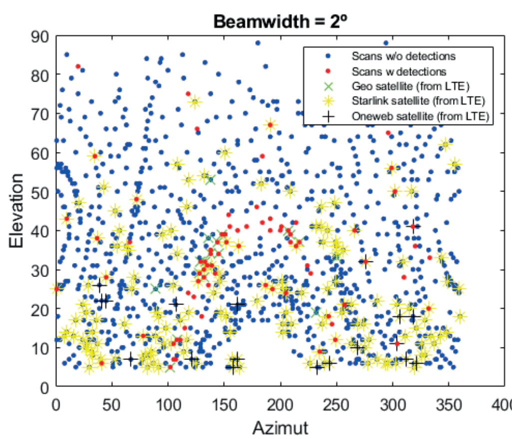

Fig. 6 Total number of scans, with scans without SS in blue and scans with SS in red. Scans with the presence of any satellite crossing the 2° beam during the 30 seconds of the scan are in yellow (Starlink), green (GSO), and black (OneWeb).

ing the 30 seconds that each scan lasts, for all 15 channels in D-band. First, the total system noise temperature during the 24-hour IVS session is compared to the

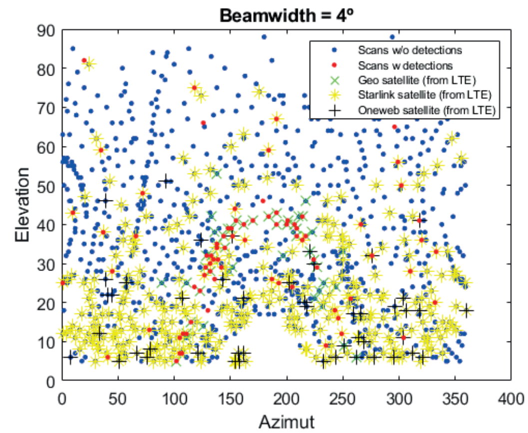

Fig. 7 Total number of scans, with scans without SS in blue and scans with SS in red. Scans with the presence of any satellite crossing the 4° beam during the 30 seconds of the scan are yellow (Starlink), green (GSO), and black (OneWeb).

total integrated power from the spectrum data. This average is computed over the 15 channels.

Figure 8 shows some strong correlation through an increase in system noise temperature with the most polluted scans. Scans 343, 439, and 385 appear to be the most polluted ones. For simplicity, only the most critical case is shown in detail in this report.

In order to compare the differences in system noise temperature between two scans (one with strong RFI and another without), two scans that are similar in both elevation angle and time are compared.

Figure 9 shows the spectrum of scan #343 (at 30° elevation) versus scan #352 (at 32° elevation). Figure 10 compares the system noise temperature of both scans. As can be seen from the graph, the scan with the strong signal from the satellite shows much higher values of T_{sys} even in the adjacent band of the satellite emission.

Additionally, Figures 11 and 12 show the comparison of the impact of the increase in T_{sys} for each D-band

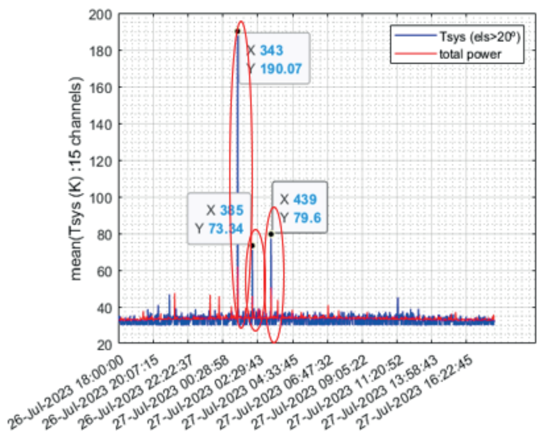

Fig. 8 A comparison of the total integrated power of the RFI vs. the mean T_{sys} along the 15 channels during the whole IVS session.

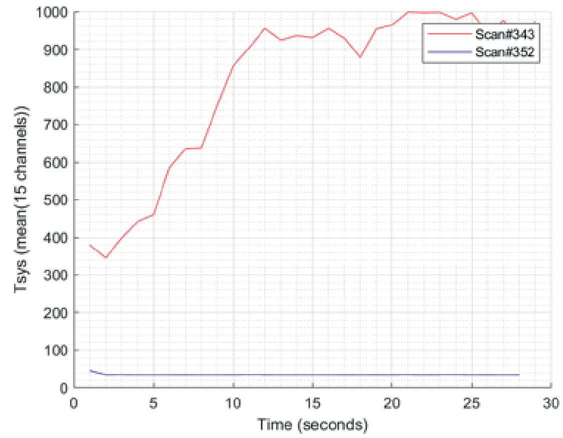

Fig. 10 Mean system noise temperature over the 15 D-band channels of two different scans.

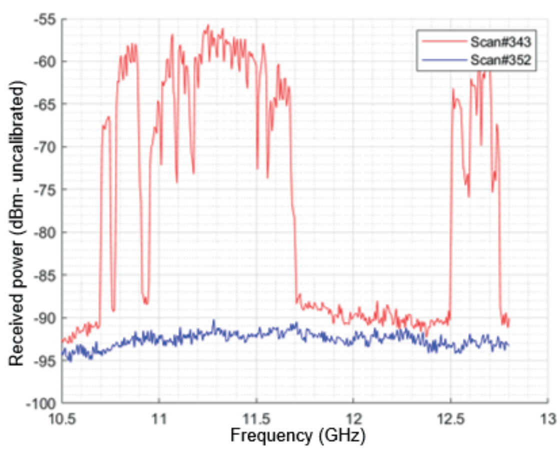

Fig. 9 Spectrum data of two different scans.

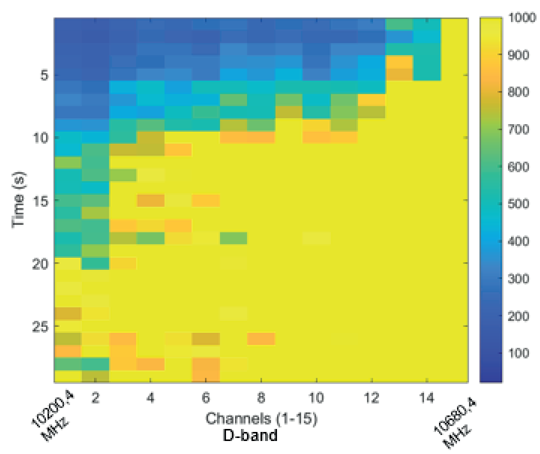

Fig. 11 $Tsys$ of the scan #343 over 30 seconds and the 15 channels in D-band.

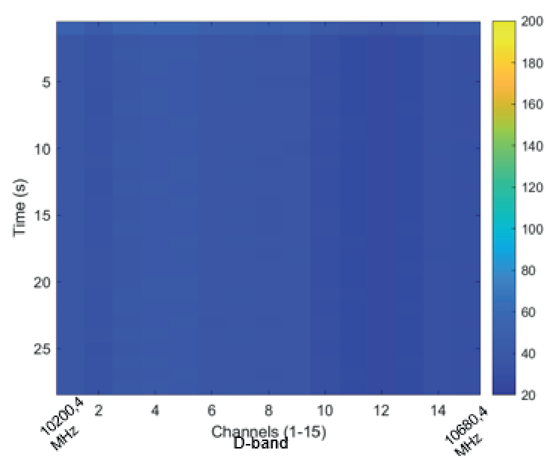

Fig. 12 $Tsys$ of the scan #352 over 30 seconds and the 15 channels in D-band.

channel in the same two scans (with RFI and without RFI from the satellite, respectively).

References

1. Di Vruno, F., Tornatore, V. (2023). Large satellite constellations and their potential impact on VGOS operations. arXiv preprint arXiv:2307.04219.
2. Technical and operational characteristics of the existing and planned Geodetic Very Long Baseline Interferometry (2022), Rep. RA.2507-2
3. B. Petrachenko, "The Impact of Radio Frequency Interference (RFI) on VLBI2010" IVS 2010 General Meeting Proceedings, p. 434–438, NASA/CP-2010-215864, 2010.